cerebral blood flow and prevention of ischemic brain injury after middle cerebral artery occlusion in rats. *J Cereb Blood Flow Metab.* 17: 19-25

16. **Watanabe K, Takayasu M, Noda A, Hara M, Takagi T, Suzuki Y, Yoshia J** 2001 Adrenomedullin reduces ischemic brain injury after transient middle cerebral artery occlusion in rats. *Acta Neurochir (Wien).* 143: 1157-1161

17. **Xia CF, Yin H, Borlongan CV, Chao J, Chao L** 2004 Adrenomedullin gene delivery protects against cerebral ischemic injury by promoting astrocyte migration and survival. *Hum Gene Ther.* 15: 1243-1254

18. **Hashida S, Kitamura K, Nagatomo Y, Shibata Y, Imamura T, Yamada K, Fujimoto S, Kato J, Morishita K, Eto T** 2004 Development of an ultrasensitive enzyme immunoassay for human proadrenomedullin N-terminal 20 peptide and direct measurement of two molecular forms of PAMP in plasma from healthy subjects and patients with cardiovascular disease. *Clin Biochem.* 37: 14-21

19. **Longa EZ, Weinstein PR, Carlson S, Cummins R** 1989 Reversible middle

cerebral artery occlusion without craniectomy in rats. *Stroke.* 20: 84-91

20. **Teramoto T, Qiu J, Plumier JC, Moskowitz MA** 2003 EGF amplifies the replacement of parvalbumin-expressing striatal interneurons after ischemia. *J Clin Invest.* 111: 1125-1132

21. **Venditti A, Battaglia A, Del Poeta G, Buccisano F, Maurillo L, Tamburini A, Del Moro B, Epiceno AM, Martiradonna M, Caravita T, Santinelli S, Adorno G, Picardi A, Zinno F, Lanti A, Bruno A, Suppo G, Franchi A, Franconi G, Amadori S** 1999 Enumeration of CD34+ hematopoietic progenitor cells for clinical transplantation: comparison of three different methods. *Bone Marrow Transplant.* 24: 1019-1027

22. **Swanson RA, Morton MT, Tsao-Wu G, Savalos RA, Davidson C, Sharp FR** 1990 A semiautomated method for measuring brain infarct volume. *J Cereb Blood Flow Metab.* 10: 290-293.

23. **Zhang ZG, Zhang L, Croll SD, Chopp M** 2002 Angiopoietin-1 reduces

cerebral blood vessel leakage and ischemic lesion volume after focal cerebral embolic ischemia in mice. *Neuroscience* 2002 113: 683-687.

24. **Hayashi H, Ishisaki A, Imamura T** 2003 Smad mediates BMP-2-induced upregulation of FGF-evoked PC12 cell differentiation. *FEBS Lett.* 536: 30-34

25. **Iimuro S, Shindo T, Moriyama N, Amaki T, Niu P, Takeda N, Iwata H, Zhang Y, Ebihara A, Nagai R** 2004 Angiogenic effects of adrenomedullin in ischemia and tumor growth. *Circ Res.* 95: 415-423

26. **Nakano S, Kogure K, Fujikura H** 1990 Ischemia-induced slowly progressive neuronal damage in the rat brain. *Neuroscience.* 38: 115-124

27. **Graham SH, Chen J** 2001 Programmed cell death in cerebral ischemia. *J Cereb Blood Flow Metab.* 21: 99-109

28. **Northington FJ, Ferriero DM, Graham EM, Traystman RJ, Martin LJ** 2001 Early Neurodegeneration after Hypoxia-Ischemia in Neonatal Rat Is Necrosis while Delayed Neuronal Death Is Apoptosis. *Neurobiol Dis.* 8: 207-219

29. **Stoll G, Jander S, Schroeter M** 1998 Inflammation and glial responses in ischemic brain lesions. *Prog Neurobiol.* 56: 149-171.

30. **Gilgun-Sherki Y, Rosenbaum Z, Melamed E, Offen D** 2002 Antioxidant therapy in acute central nervous system injury: current state. Pharmacol Rev. 54: 271-284

31. **Kim W, Moon SO, Lee S, Sung MJ, Kim SH, Park SK** 2003 Adrenomedullin reduces VEGF-induced endothelial adhesion molecules and adhesiveness through a phosphatidylinositol 3'-kinase pathway. *Arterioscler Thromb Vasc Biol.* 23: 1377-1383

32. **Kawai J, Ando K, Tojo A, Shimosawa T, Takahashi K, Onozato ML, Yamasaki M, Ogita T, Nakaoka T, Fujita T** 2004 Endogenous adrenomedullin protects against vascular response to injury in mice. *Circulation.* 109: 1147-1153

33. **Niu P, Shindo T, Iwata H, Iimuro S, Takeda N, Zhang Y, Ebihara A, Suematsu Y, Kangawa K, Hirata Y, Nagai R** 2004 Protective effects of

endogenous adrenomedullin on cardiac hypertrophy, fibrosis, and renal damage. *Circulation.* 109: 1789-1794

34. **Krupinski J, Kaluza J, Kumar P, Kumar S, Wang JM** 1994 Role of angiogenesis in patients with cerebral ischemic stroke. *Stroke.* 25: 1794-1798

35. **Palmer TD, Willhoite AR, Gage FH** 2000 Vascular niche for adult hippocampal neurogenesis. *J Comp Neurol.* 425: 479-494

36. **Louissaint A Jr, Rao S, Leventhal C, Goldman SA** 2002 Coordinated interaction of neurogenesis and angiogenesis in the adult songbird brain. *Neuron.* 34: 945-960

37. **Asahara T, Murohara T, Sullivan A, Silver M, van der Zee R, Li T, Witzenbichler B, Schatteman G, Isner JM** 1997 Isolation of putative progenitor endothelial cells for angiogenesis. *Science.* 275: 964-967

38. **Taguchi A, Soma T, Tanaka H, Kanda T, Nishimura H, Yoshikawa H, Tsukamoto Y, Iso H, Fujimori Y, Stern DM, Naritomi H, Matsuyama T** 2004

Administration of CD34+ cells after stroke enhances neurogenesis via angiogenesis in a mouse model. *J Clin Invest.* 114: 330-338

39. **Nagaya N, Satoh T, Nishikimi T, Uematsu M, Furuichi S, Sakamaki F, Oya H, Kyotani S, Nakanishi N, Goto Y, Masuda Y, Miyatake K, Kangawa K** 2000 Hemodynamic, renal, and hormonal effects of adrenomedullin infusion in patients with congestive heart failure. *Circulation.* 101: 498-503

40. **Doi K, Itoh H, Ikeda T, Hosoda K, Ogawa Y, Igaki T, Yamashita J, Chun TH, Inoue M, Masatsugu K, Matsuda K, Ohmori K, Nakao K** 1997 Adenovirus-mediated gene transfer of C-type natriuretic peptide causes G1 growth inhibition of cultured vascular smooth muscle cells. *Biochem Biophys Res Commun.* 239: 889-894

41. **Komatsu Y, Itoh H, Suga S, Ogawa Y, Hama N, Kishimoto I, Nakagawa O, Igaki T, Doi K, Yoshimasa T, Nakao K** 1996 Regulation of endothelial production of C-type natriuretic peptide in coculture with vascular smooth muscle cells.

Role of the vascular natriuretic peptide system in vascular growth inhibition. *Circ Res.* 78: 606-614

42. **Hippenstiel S, Witzenrath M, Schmeck B, Hocke A, Krisp M, Krull M, Seybold J, Seeger W, Rascher W, Schutte H, Suttorp N** 2002 Adrenomedullin reduces endothelial hyperpermeability. *Circ Res.* 91: 618-625

43. **Nakatomi H, Kuriu T, Okabe S, Yamamoto S, Hatano O, Kawahara N, Tamura A, Kirino T, Nakafuku M** 2002 Regeneration of hippocampal pyramidal neurons after ischemic brain injury by recruitment of endogenous neural progenitors. *Cell.* 110: 429-441

44. **Zhang ZG, Zhang L, Jiang Q, Zhang R, Davies K, Powers C, Bruggen N, Chopp M** 2000 VEGF enhances angiogenesis and promotes blood-brain barrier leakage in the ischemic brain. *J Clin Invest.* 106: 829-838

45. **Shimamura M, Sato N, Oshima K, Aoki M, Kurinami H, Waguri S, Uchiyama Y, Ogihara T, Kaneda Y, Morishita R** 2004 Novel therapeutic strategy

to treat brain ischemia: overexpression of hepatocyte growth factor gene reduced ischemic injury without cerebral edema in rat model. *Circulation.* 109: 424-431

46. **Sun Y, Jin K, Xie L, Childs J, Mao XO, Logvinova A, Greenberg DA** 2003 VEGF-induced neuroprotection, neurogenesis, and angiogenesis after focal cerebral ischemia. *J Clin Invest.* 111: 1843-1851

47. **Sondell M, Lundborg G, Kanje M** 1999 Vascular endothelial growth factor has neurotrophic activity and stimulates axonal outgrowth, enhancing cell survival and Schwann cell proliferation in the peripheral nervous system. *J Neurosci.* 19: 5731-5740

Tables:

Table 1: Plasma concentrations of human AM and systolic blood pressure in Wt and three lines of AM-Tg mice.

	Wt	Low conc.	Medium conc.	High conc.
Total AM (fmol/ml)	1.1±0.2	17.6±4.4**	142.2±18.4**	585.5±117.7**
Mature AM (fmol/ml)	0.5±0.4	2.6±0.6**	10.4±2.4**	24.9±4.2**
Systolic BP (mmHg)	122.7±1.6	113.0±2.5**	113.4±2.6**	109.4±2.5**

**, $P<0.01$ versus Wt; n=4-12

Table 2: Significant correlation between the regenerative elements and apoptosis, neurogenesis, and functional recovery after 20m-MCAO.

X	Y	Regression line	P
Capillary density (% field)	Apoptotic cells (/mm^2)	Y=-2.3X+37	0.01
Capillary density (% field)	Regenerated neuron (/mm^2)	Y=3.2X-21	0.003
Capillary density (% field)	Rota-rod result (second)	Y=1.3X+9	0.005
Regenerated neuron (/mm^2)	Rota-rod result (second)	Y=0.3X+19	0.08

n=12-24

Table 3: Comparison of the effects on neuro-protection and vascular regeneration after 20m-MCAO between Wt control mice, hydralazine-administrated mice, and the low and high conc. lines of AM-Tg.

Mice	Infarct area (mm^2/field)	Brain blood flow (%contralateral)	Systolic BP (mmHg)
Control	0.90±0.09	80.8±2.3	120.1±2.2
Hydralazine	0.94 ± 0.17^{ns}	79.6 ± 2.6^{ns}	$101.0\pm3.9^{**}$
Low-conc. AM-Tg	$0.58\pm0.12^{*}$	$88.4\pm2.9^{*}$	$105.1\pm1.8^{**}$
High-conc. AM-Tg	$0.67\pm0.09^{*}$	$86.3\pm2.0^{*}$	$106.4\pm3.5^{**}$

*, $P<0.05$; **, $P<0.01$; ns, not significant versus control; n=6

Table 4: Effects of AM-antagonists, PKA inhibitors, and PI3K inhibitors on AM-induced neural differentiation of PC12 cells.

	Process length (μm/cell)		Process length (μm/cell)
PC12	6.8±1.7	PC12+AM+Rp-cAMP10^{-5}mol/l	$10.2\pm2.7^{**}$
PC12+AM10^{-8}mol/l	$23.6\pm4.0^{††}$	+AM+PKA Inh.10^{-6}mol/l	$7.2\pm2.3^{**}$

+AM+AM(22-52)10^{-5}mol/l	11.8±3.4**	+AM+LY294002 10^{-5}mol/l	4.6±1.6**
+AM+CGRP(8-37)10^{-5}mol/l	14.8±1.9*	+AM+Wortmannin 10^{-7}mol/l	5.4±1.1**
		PC12 - EC co-culture	20.7±2.1††

EC, endothelial cell; ††, P<0.01 versus PC12 without AM; *, P<0.05; **, P<0.01 versus PC12 with AM 10^{-8} mol/l; n=8

Figure legends

Figure 1: Generation of transgenic mice which overproduce AM but do not overproduce mature PAMP in the liver and augmented angiogenesis in the transgenic mice after femoral artery occlusion. A: Schematic representation of the transgene construct derived from human AM gene cDNA with a point mutation in the amidation signal of PAMP. B: Southern blot analysis of the tail DNA of the founder mice. Arrow: blots for the transgene. Internal controls for indicated copies are located in the left three lanes. The line No. indicates the mice in which the transgene was detected by polymerase chain reaction (PCR). The copy numbers estimated by densitometry and the plasma concentrations of total human AM in F3 mice of the lines are shown. C: Hindlimb blood flow analyzed by LDPI. Red or white indicates a higher flow than blue or green. Arrows: Comparison of ischemic hindlimbs between Wt and AM-Tg on day 28 after femoral artery ligation. D: Quantitative analysis of the hindlimb blood

flow in ischemia. *, P<0.05 for Wt versus AM-Tg by ANCOVA analysis; n=6.

Figure 2: Effects of AM on infarct area and gliosis after the non-fatal stroke, 20m-MCAO. A: Histological examination of the ischemic striatum. The outlined field was examined for infarct area and gliosis. The ischemic side and contralateral side on day 3 after 20m-MCAO are shown. Scale bar, 500μm (x5 magnification) B and C: Representative images of the ischemic striatum on postoperative day 7 stained for NeuN (Blue) and GFAP (Green). Infarct area, defined as the region where NeuN immunoreactivity was lost, and gliosis, defined as the area where GFAP immunoreactivity was observed, in Wt (B) and AM-Tg (C) are shown. Scale bar, 500μm (x5 magnification) D and E: Quantitative analysis of the infarct area (D) and gliosis (E) *, P<0.05; ns, not significant for Wt versus AM-Tg; n=12.

Figure 3: Effects of AM on leukocyte infiltration, ROS production, and apoptosis in the ischemic brain after 20m-MCAO. A and B: Detection of leukocyte infiltration in the ischemic core on postoperative day 7 by immunostaining for $CD45^+$ cells (red) in Wt (A) and AM-Tg (B). Arrows: $CD45^+$ cells. C and D: in situ detection of ROS in ischemic striatum on postoperative day 7 by immunostaining for dihydroethidium (diHE; red) in Wt (C) and AM-Tg (D). E and F : Detection of apoptotic cells in the ischemic core on postoperative day 7 by immunostaining for $ssDNA^+$ cells (green) in Wt (E) and AM-Tg (F). Arrows, $ssDNA^+$ cells. G and H: Quantitative analysis of $CD45^+$ cells (G) and $ssDNA^+$ cells (H) in the ischemic core. *, $P<0.05$; **, $P<0.01$; ns, not significant for Wt versus AM-Tg; n=12. Scale bar, 100μm (x20 magnification).

Figure 4: Effects of AM on vascular regeneration in the ischemic brain after 20m-MCAO. A-D: Analysis of the blood flow in the ischemic brain by LDPI

evaluated in mice with the scalp removed (A). Flowmetric analysis of the ischemic brain during MCA-Occlusion (B) and on day 28 after 20m-MCAO in Wt (C) and AM-Tg (D). Red or white indicates higher flow than blue or green. E-G: Histological examination of the vasculature in the ischemic core with PECAM-1 staining. Ischemic striatum on day 28 after 20m-MCAO in Wt (E) and AM-Tg (F), and contralateral non-ischemic striatum (G). Scale bar, 100μm (x20 magnification). H: Quantitative analysis of the blood flow in the ischemic brain. Comparison of recovery from ischemia after 20m-MCAO between Wt and AM-Tg. MCA-Oc, blood flow during MCA occlusion; **, $P<0.01$ for Wt versus AM-Tg by ANCOVA analysis; n=8. I: Quantitative analysis of capillary density in the ischemic brain. Comparison of time course for increase in capillary density, determined as the number of PECAM-1^+ cells, between Wt and AM-Tg mice. *, $P<0.05$; ns, not significant; n=8.

Figure 5: Effects of AM on mobilization of $CD34^+$ mononuclear cells into peripheral blood after 20m-MCAO. A-C: Quantification of $CD34^+$ mononuclear cells after 20m-MCAO. Scatter plots for FACS analysis of the $CD34^+$ cells in peripheral blood of Wt (A) and AM-Tg (B) on postoperative day 3. Yellow: $CD34^+$ - CD45dim mononuclear cells. Comparison of the time course for mobilization of $CD34^+$ cells into peripheral blood between Wt and AM-Tg (C). *, $P<0.05$; ns, not significant; n=6.

Figure 6: Effects of AM on neurogenesis and recovery of impaired motor function after 20m-MCAO. A and B: Detection of regenerated neurons on postoperative day 56 by immunostaining for BrdU and NeuN. Arrows, BrdU - NeuN double positive cells in the ischemic core of Wt (A) and AM-Tg (B). Scale bar, 100μm. C: Quantitative analysis of regenerated neurons. *, $P<0.05$; ns, not significant; n=12. D: Recovery of impaired motor function after

20m-MCAO, quantified as the exercise time on an accelerating rota-rod from the start to collapse down. *, $P<0.05$; **, $P<0.01$ for Wt versus AM-Tg by ANCOVA analysis; n=14.

Figure 7: Effects of AM on infarct size and brain edema in the fatal stroke, 2h-MCAO. A: Comparison of infarct size between Wt and AM-Tg with TTC staining at 4.0mm from the frontal pole. White area represents infarction. B and C: Infarct (B) and edema (C) volumes quantified 24 hours after the operation of 2h-MCAO. *, $P<0.05$; ns, not significant for Wt and AM-Tg; n=9. D: Representative image of in situ Evans Blue leakage into the ischemic core at 24 hours after 2h-MCAO. E: Quantification of Evans Blue in the ischemic brain. **, $P<0.01$; n=4.

Figure 8: Effects of AM in vitro on apoptosis of NHNP neuronal progenitor cells

and neuronal differentiation of PC12 cells. A-D: In vitro analysis of apoptotic neuro-progenitor cells (NHNP) after incubation with (B) or without (A) AM. NHNP cell number (C) and the ratio of ssDNA$^+$ cells to total cells (D) after 48 hours incubation. *, $P<0.05$; **, $P<0.01$; ns, not significant versus control; n=4; scale bar, 100μm. E-G: Effects of AM on neuronal differentiation of PC12 cells evaluated by the length of neuronal process. Microscopic examination of PC12 cells after incubation for 7 days (E). AM (F) or NGF (G) was added to the culture medium. Quantification of cell number (H) and the length of neuronal process (I). *, $P<0.05$; **, $P<0.01$; ns, not significant; n=6; scale bar, 100μm.

Figure 9: Effects of exogenously administrated AM on neuro-protection and vascular regeneration after 20m-MCAO. 50 ng/h AM was administrated to mice with an intra-peritoneally implanted osmotic pump. Infarct area (A) and blood flow (B) on postoperative day 7 with different starting points for AM

administration. *, P<0.05; **, P<0.01; ns, not significant versus vehicle; n=6.

Figure 10: Summary of "Brain remodeling" after ischemia and effects of AM on the ischemic brain observed in this study.

Figure 1

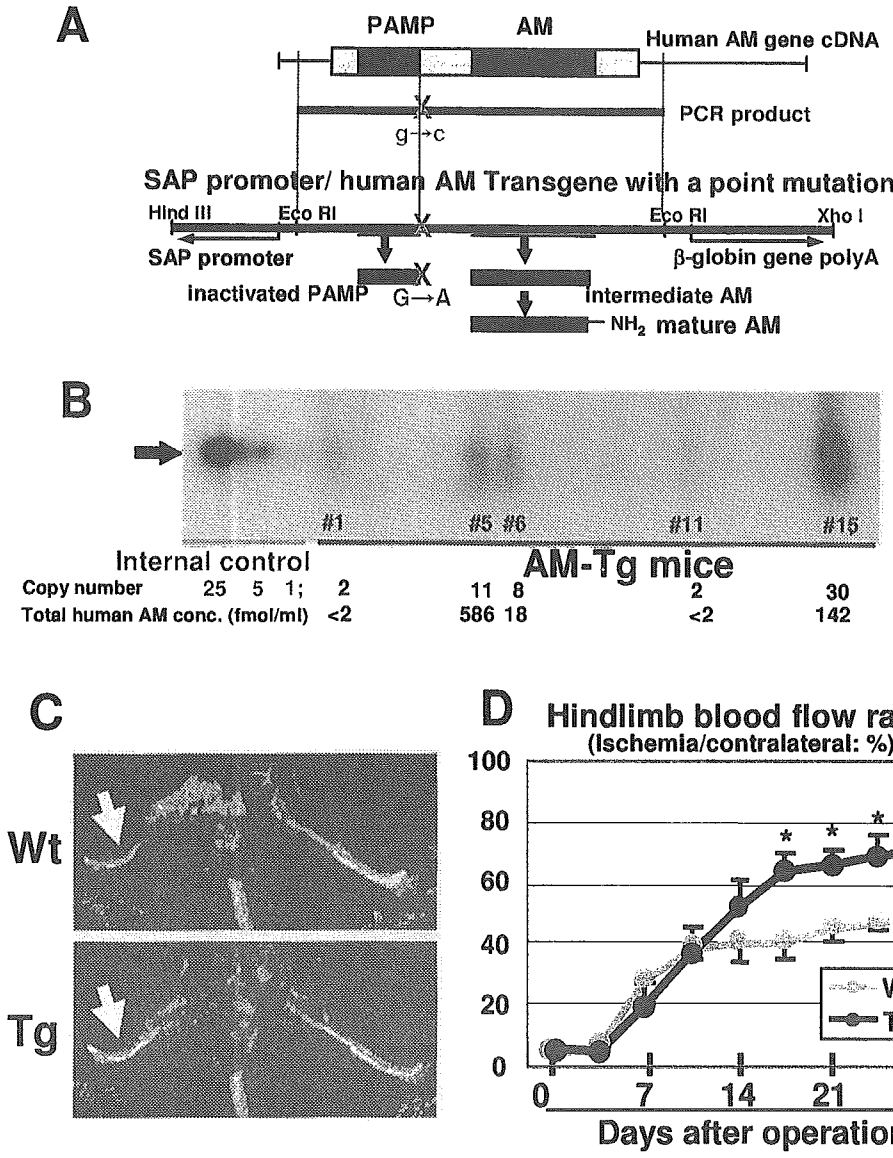
A
PAMP
AM
Human AM gene cDNA
PCR product
g→c
SAP promoter/ human AM Transgene with a point mutation
Hind III
Eco RI
Eco RI
Xho I
SAP promoter
β-globin gene polyA
inactivated PAMP
G→A
Intermediate AM
NH2 mature AM
B
#1
#5 #6
#11
#15
Internal control
AM-Tg mice
Copy number 25 5 1; 2 11 8 2 30
Total human AM conc. (fmol/ml) <2 586 18 <2 142
C
Wt
Tg
D
Hindlimb blood flow ratio
(Ischemia/contralateral: %)
100
80
60
40
20
0
0 7 14 21 28
Days after operation
Wt
Tg